J Mater Sci (2019) 54:3262–3272

Energy materials

Effect of biomass on reaction performance of sintering fuel

Chao Liu[1], Yuzhu Zhang[1,*], Kai Zhao[1], Hongwei Xing[1], and Yue Kang[1]

[1] College of Metallurgy and Energy, North China University of Science and Technology, Tangshan 063009, People's Republic of China

Received: 26 June 2018
Accepted: 22 October 2018
Published online: 31 October 2018

© Springer Science+Business Media, LLC, part of Springer Nature 2018

ABSTRACT

Sintering flue gas is the main source of air pollution in the iron and steel industry. Facing stringent emission standards set to limit the amount of flue gas pollutants, multi-pollutant control in sintering flue gas has become a necessity in the iron and steel industry. Utilizing biomass fuel with low S and N contents to replace a portion of coke in the sintering process can offer control at the source of sintering flue gas pollutants. This study is aimed at elucidating the reaction mechanism of mixed fuel in the sintering process using thermogravimetric experiments of the combustion and gasification reactions. The results show that the reaction performance of biomass fuel is better than that of coke. In addition, biomass fuel can improve the reaction performance of mixed fuel. When the content of biomass fuel increased from 20 to 80%, the temperatures of both the combustion and gasification reactions decreased, the weight loss rate of the mixed fuel increased, and the gap between the calculated and experimental values widened. By studying the reaction mechanism of mixed fuel, we found that the sintering fuel reactivity increases mainly because the porous structure of biomass fuel provides a large specific surface area for the combustion or gasification reaction, and the alkali metals, K and Na, in the biomass fuel act as catalysts to the reaction.

Introduction

In recent years, air pollution has become an increasingly serious issue, drawing attention to the iron and steel industry, which is a major polluter. The sintering process emits more than 40% of the dust, 70% of the SO_2, and 50% of the NO_x emitted by exhaust gases. Therefore, relevant government departments have formulated atmospheric emission standards for the iron and steel industry and put forward ultra-low emission limits to strictly control the emissions of pollutants such as SO_2 and NO_x. More than 90% of the NO_x produced in the sintering process originates from nitrogen compounds in the fuel. The SO_2 in sintering flue gas is mainly produced by the reaction between O and S in fuel, where it is generally believed that the ratio of S to SO_2 can reach 85–95%. The CO_x in sintering flue gas originates from the

Address correspondence to E-mail: zyz@ncst.edu.cn

https://doi.org/10.1007/s10853-018-3061-2

combustion of sintering fuel. Hence, most of the CO_x, NO_x and SO_2 pollutants are derived from the sintering fuel [1, 2]. Biomass fuel is also used in the sintering process, where CO_2 is produced and takes part in the atmospheric carbon cycle. Biomass fuel has low S and low N, which can reduce the emission of SO_2 and NO_x from the sintering source [3, 4]. Therefore, utilizing biomass coal with low S and N can offer control at the source of pollutants released by sintering flue gas.

At present, the application of biomass fuel in sintering production has been studied by a number of researchers. Fan et al. [5] studied the effect of replacing coke with biomass fuels on sintering technical indexes and sinter properties. The results show that when biomass fuels replace 40% of coke breeze, the speed of sintering is increased, while the finished product ratio and the drum strength of sinters are decreased. Kawaguchi et al. [6] studied optimization of the process through size and moisture control of the biomass char. Biomass carbonized char is evaluated based on sinter yield, similar to anthracite or coke. The use of biomass char is effective at decreasing CO_2, NO_x, SO_x, and dust emissions in sinter exhaust gas. Zandi et al. [7] characterized and prepared olive residues, sunflower husk pellets, almond shells, hazelnut shells, and Bagasse pellets for sintering. A laboratory sinter pot was used to study the sintering behavior of biomass material. Ooi et al. [8] used a laboratory-scale sintering reactor, or pot was employed to determine the effect of charcoal combustion on iron ore sintering performance and emission of persistent organic pollutants. Many scholars have studied the effect of using biomass fuel (instead of coke) on the sintering process and fuel gas pollutant reduction. However, the mechanism of sintering mixed fuel is seldom studied. In this paper, we compare the combustion and gasification reactivity of biomass fuel, coke, and mixed fuel and provide insight into the mechanism behind the reaction performance of biomass fuel on sintering mixed fuel, which provides theoretical guidance for sintering production with reasonable addition of biomass fuel.

Materials and methods

Materials

The biomass fuel in the experiment is homemade charcoal [9], and the coke is a sintering fuel provided by a sintering plant. The proximate analysis and calorific value of fuels are shown in Table 1.

Thermogravimetric analysis

Thermogravimetric analysis (TG, SETSYS Evolution) was used to perform the combustion and gasification reaction experiments at atmospheric pressure. The temperature of the sample was raised to 383 K for 2 min at a heating rate of 10 K/min in high purity N_2 (100 mL/min) to remove moisture. Soon afterward, the experimental atmosphere was changed from N_2 to air or CO_2 (50 mL/min) for the combustion reaction or gasification reaction. When the flue gas analyzer showed that the air or CO_2 content was close to 100%, the temperature of the sample was increased to the required temperature at a heating rate of 10 K/min. The sample was placed in an alumina crucible (φ 5 mm × 8 mm), the mass of sample was 10 ± 0.5 mg, and the particle size of the sample was less than 200 mesh. All experimental data were corrected by a blank test under the same operating conditions to eliminate the effect of buoyancy during the experiment. The experimental data were used to calculate the activation energy (E) and the pre-exponential factor (A). The experimental program is shown in Table 2.

In order to study the effect of biomass fuel on the reactivity of sintering fuel, the TG experimental and calculated weight loss curves and the DTG experimental and calculated weight loss rate curves of mixed fuel were compared in the combustion and gasification experiments. TG and derivative TG (DTG) data were calculated for mixed fuel using Eqs. (1) and (2):

$$TG_{calc} = \omega_{char} TG_{char} + \omega_{coke} TG_{coke} \quad (1)$$

$$DTG_{calc} = \omega_{char} DTG_{char} + \omega_{coke} DTG_{coke} \quad (2)$$

where TG_{calc} is the calculated value of mixed fuel, mg; ω_{char} and ω_{coke} are the mass fraction of charcoal and coke separately, %. The calculated value is a weighted average of the data obtained by the two fuels independently.

Table 1 Proximate analysis and calorific value of fuels

Type	Volatile matter (%)	Fixed carbon (%)	Ash (%)	Moisture (%)	Calorific value (MJ/kg)
Coke	1.62	83.21	14.80	0.37	26.16
Charcoal	5.02	87.60	5.88	1.50	27.61

Table 2 Experimental scheme for fuel reaction performance

Group	Coke	Charcoal	Heating rate	Atmosphere
1	100%	–	B = 10 K/min	Combustion reaction: 21% O_2 + 79% N_2
2	–	100%		Gasification reaction: 100% CO_2
3	50%	50%		
4	80%	20%		
5	20%	80%		

Kinetic theoretical analysis

The reactivity of fuel is determined by the reaction rates (k) of fuels. Based on the results of previous studies [10–12], the reaction of chars has generally been described as a global one-step kinetic chemical reaction model. The rate constant (k) was calculated according to Eq. (3):

$$\frac{d_\alpha}{d_t} = k \cdot (1-\alpha) \tag{3}$$

where α is the fractional weight conversion, $\alpha = (1 - m/m_0)$, m is the residual sample weight, mg, and m_0 is the original sample weight, mg. Equation (4) is obtained by rearranging Eq. (3). Equation (5) is the integrated solution of Eq. (4) subject to the initial condition (a = 0, t = 0). The rate constant (k) can be obtained as the negative slope between $\ln(1-\alpha)$ and the reaction time(t).

$$k = \frac{d_\alpha}{d_t} \cdot \frac{1}{1-\alpha} \tag{4}$$

$$k \cdot t = -\ln(1-\alpha) \tag{5}$$

The activation energy (E) and a pre-exponential factor (A) can be obtained via the Arrhenius equation as shown in Eq. (6). Combining Eqs. (3) and (6) leads to Eq. (7).

$$k = A \cdot \exp(-E/RT) \tag{6}$$

$$\frac{\partial_\alpha}{\partial_t} = A \cdot \exp\left(-\frac{E}{RT}\right)(1-\alpha) \tag{7}$$

where R is the gas constant (8.314 J K^{-1} mol^{-1}) and T is the temperature, K. Some scholars [13, 14] find that the Coats–Redfern approximation to the temperature integral is both simple and accurate, so the Coats–Redfern approximation was used to calculate the relevant parameters. In the non-isothermal analysis, the heating rate is a constant, resulting in Eq. (8):

$$\ln\left(\frac{-\ln(1-\alpha)}{T^2}\right) = \ln\left(\frac{AR}{\beta E}\right) - \frac{E}{RT} \tag{8}$$

where β is the heating rate, E can be obtained as the negative slope between $\ln(\ln(1-\alpha)/T^2)$ and $1/RT$, and A can be obtained as the intercept of Eq. (8).

Alkali metal detection

The morphology of samples was assessed by scanning electron microscopy on a field emission scanning electron microscope (S-4800). The alkali metals of samples in SEM images were detected by energy-dispersive spectrometer (EDS). The content of alkali metal is determined by the detection of EDS in different fuels.

Sintering pot experiment of biomass fuel

The experimental material was supplied by a Steel Corp sintering plant in Tangshan, the chemical composition of sintering material is shown in Table 3, the sintering pot experiment was carried out according to the ratio of sintering material, the basicity of sinter was 1.9, and the carbon content was 4.5%.

The chemical composition of sintering raw materials is shown in Table 3. We used an equal fixed carbon content of charcoal to replace the coke powder in the sintering experiments. The suction of ignition was 8 kPa through the bed, and the suction was

Table 3 The chemical composition of sintering raw materials (mass percent, %)

Sintering raw materials	The chemical composition						
	TFe	FeO	SiO_2	CaO	MgO	Al_2O_3	TiO_2
Iron ore	60.65	5.08	4.26	2.62	0.75	1.74	0.15
limestone	0.12	0.12	2.72	47.56	3.77	0.72	0.30
Lime	0.26	0.18	3.52	72.33	4.52	1.00	0.048
Dolomite	0.31	0.20	1.38	29.61	21.85	0.18	0.002

maintained during a 90-s ignition period. The ignition temperature (1473 K) was achieved by adjusting the flow rates of LPG and air. After ignition, the LPG/air flow was stopped, and the sintering suction raised to 12 kPa and lasted until the end of sintering. The sintering experiments scheme is shown in Table 4.

Results and discussion

Effect of biomass fuel on combustion reactivity of fuels

As shown in Fig. 1, the TG and DTG curves of combustion reaction for charcoal, coke, and mixed fuel (charcoal/coke = 50:50) were obtained by the experiments of thermogravimetric analysis.

As shown in Fig. 1a, the start and end reaction times of charcoal combustion were 35 min and 50 min, respectively, which were shorter than those of coke combustion, which were 57 min and 85 min, respectively. Hence, the reaction duration of coke was longer than that of charcoal. As shown in Fig. 1b, the DTG_{max} of the charcoal combustion reaction was about 0.78 mg min^{-1}, which is faster than that for coke, which was 0.59 mg min^{-1}. According to the TG and DTG curves for the combustion reaction, the reactivity of charcoal is obviously superior to that of coke. When charcoal was used to replace a portion of coke in the sintering process, the reactivity of fuel changed. The TG_{calc} and DTG_{calc} of mixed fuel were obtained by Eqs. (1) and (2). As shown in Fig. 1, the TG_{calc} and DTG_{calc} curves for mixed fuel are not

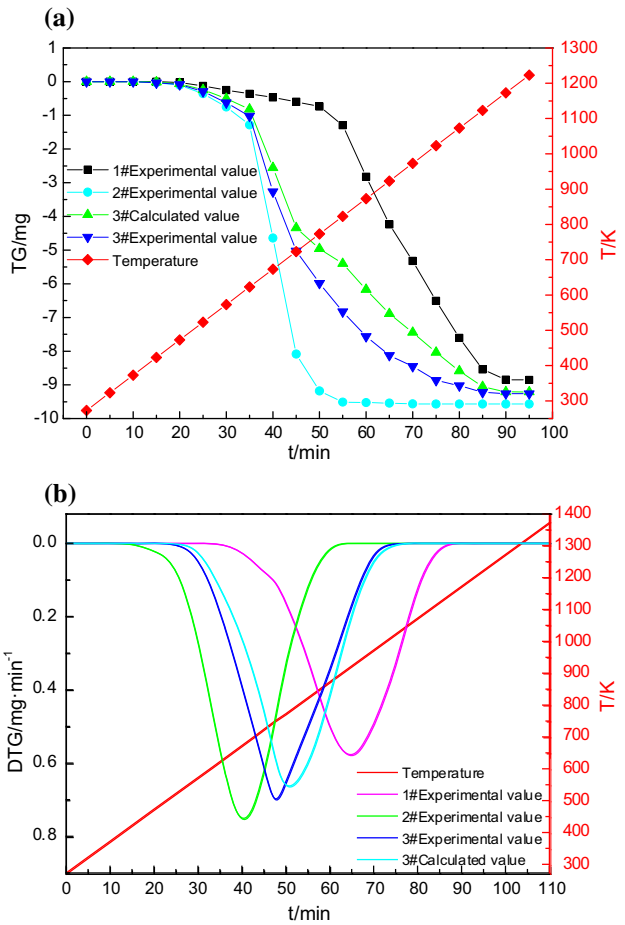

Figure 1 Combustion reactivity of fuels. **a** TG curves of fuels with different types. **b** DTG curves of fuels with different types.

identical to the experimental data. The experimental and calculated start times for the combustion reaction of mixed fuel were basically same; however,

Table 4 The ratio of the sintering experiment scheme (mass fraction/ %)

Groups	Iron ore	limestone	Lime	Dolomite	Coke	Charcoal
1	83.86	3.00	3.83	4.81	100	0
2					80	20
3					60	40
4					40	60

differences appeared, where the experimental values of weight loss tended toward those of the charcoal weight loss, while the calculated values were the averages of the coke and charcoal weight loss curve. In addition, the experimental combustion time of the mixed fuel was shorter than the calculated value. Meanwhile, the predicted value of DTG_{max} was 0.66 mg min^{-1}, which was slower than the experimentally determined DTG_{max} of 0.72 mg min^{-1}. The experimental results show that biomass fuel can, to some extent, improve the reaction performance of mixed fuel.

In order to further study the effect of biomass addition on the combustion reactivity of mixed fuels, TG and DTG experiments were carried out on different biomass fuels, as shown in Fig. 2.

Figure 2 shows the weight loss curves for the combustion reaction of mixed fuels with different ratios of charcoal. The experimental results showed that the higher the charcoal content, the earlier the fuel combustion starts, and the faster the weight loss rate of mixed fuel combustion. When the content of charcoal was increased from 20 to 80%, the reaction time of mixed fuel decreased from 85 min to 50 min, and the DTG_{max} increased from 0.58 to 0.72 mg min^{-1}. By comparing the experimental values with the predicted values, it can be found that as the biomass fuel content increases, the gap between experimental and calculated values of combustion weight loss of the mixed fuel increased. The thermogravimetric experiments show that the combustion reaction performance of the mixed fuel is not the weighted average of the two fuels, but rather the biomass fuel has a certain catalytic synergistic effect on the combustion reaction of the mixed fuel.

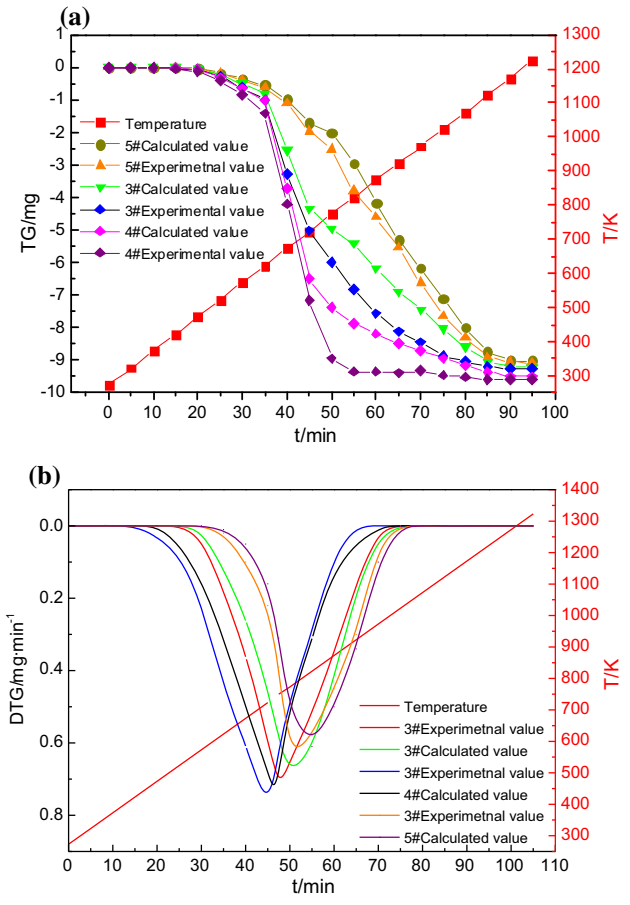

Figure 2 The combustion reactivity of mixed fuels; **a** the TG curve of fuels with different ratios, **b** the DTG of fuels with different ratios.

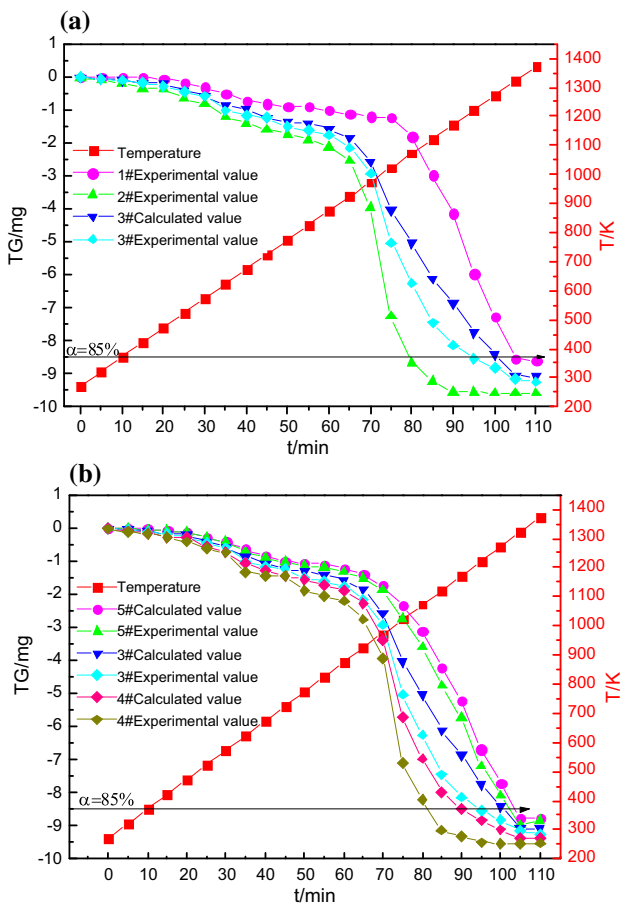

Figure 3 Gasification reactivity of fuels. **a** TG curves of fuels with different types; **b** TG curves of fuels with different ratios.

Effect of biomass fuel on gasification reactivity of fuels

Figure 3 shows the TG and DTG curves of the gasification reaction for charcoal, coke, and mixed fuel.

Removing the effect of ash in the fuel, the gasification reaction performance was compared by selecting the kinetic parameters of the conversion rate (α) of 85%. Figure 3 shows that the fuel weight loss curve is divided into two stages. In the first stage, the removal of moisture and volatile matter from the fuel resulted in weight loss. The volatile matter in the charcoal was higher than that in the coke, so the weight loss of the fuel increased with an increase in charcoal content. In the second stage, the weight loss rate sharply increased, mainly due to the fixed-carbon gasification reaction in the fuel. Faster weight loss rates occurred with increasing charcoal content. Interestingly, in the gasification reaction experiment, the calculated weight losses were not same as the experimental weight losses. The gap between TG_{calc} and TG_{exp} increased with the increase in charcoal content in the mixed fuel, showing that the charcoal also has a catalytic synergistic effect on the gasification reaction of mixed fuel.

According to the weight loss curve of the fuel gasification reaction, the kinetic parameters were calculated by the Coats–Redfern approximation method to explain the catalytic synergistic effect of biomass fuel on coke. Figure 4 shows the relationship between $\ln(\ln(1-\alpha)/T^2)$ and 1/RT, where the activation energy was obtained from the negative slope, and the pre-exponential factor was obtained from the intercept. The kinetic parameters of the fuel gasification reaction are shown in Table 5.

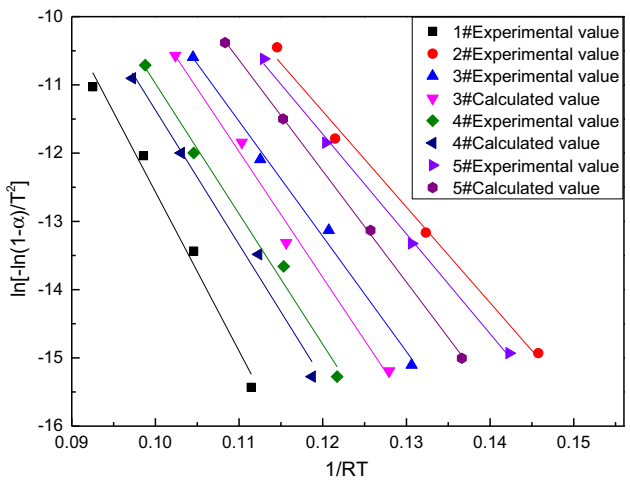

Figure 4 The relationship between $\ln(\ln(1-\alpha)/T_2)$ and $1/RT$.

Combining Fig. 3 and Table 5, we find that the slope of the TG curve for coke was largest, and the slope for charcoal was smallest. In addition, as the charcoal content in the mixed fuel increased, the slope of the curve approached that of charcoal. By comparing the kinetic parameters of the fuel in gasification reaction (Table 3) with the increase in charcoal content in fuel (20–80%), we see that the pre-exponential factor increased from 2.8×10^5 to 4.7×10^6 s^{-1}, the activation energy decreased from 191.08 to 156.84 $kJ \cdot mol^{-1}$, and the gap between experimental and calculated values of the pre-exponential factor or activation energy increased. The results also confirmed that the gasification reaction performance of mixed fuel is not only the weighted average of two fuels, but that charcoal has a certain catalytic synergistic effect on the gasification reaction performance of mixed fuel, where the higher the charcoal content in mixed fuel, the greater the effect.

Mechanism behind the influence of biomass fuel on the reactivity of coke

A field emission scanning electron microscope (S4800) was used to study the original surfaces of coke and charcoal. The microstructure of coke and charcoal is shown in Fig. 5. Coke and charcoal samples were also analyzed using an automatic QUADRASORB specific surface area and pore diameter analyzer. The specific surface area and pore diameter distribution of the fuels were calculated by the Brunauer–Emmett–Teller (BET) method, according to the adsorption isotherm. These results are shown in Table 6.

Observations of the microstructure of fuel in Fig. 5 show that the charcoal was more porous than coke and had more uniform pore size distribution. The specific surface area, pore volume, and pore size distribution of coke and charcoal (Table 4) were used to find that the specific surface area of charcoal was 30.628 m^2/g and the pore volume of charcoal was about four times that of coke. The pore size of charcoal was about half that of coke, which indicated that the surface structure of charcoal was loose and porous, and the porosity of charcoal was smaller and greater than that of coke. The microstructure of charcoal provided more opportunity to be in contact with the reaction gas for the combustion or

Table 5 Kinetic parameters of fuels using Coats–Redfern approximations

Group	A_1 (s^{-1})	A_2 (s^{-1})	ΔA (s^{-1})	E_1 (kJ mol^{-1})	E_2 (kJ mol^{-1})	ΔE (kJ mol^{-1})
1	–	1.3×10^7	–	–	233.23	–
2	–	3.9×10^4	–	–	140.27	–
3	2.7×10^5	8.8×10^5	6.1×10^5	186.75	168.70	− 18.05
4	7.8×10^5	4.7×10^6	3.9×10^6	214.63	191.08	− 23.55
5	1.8×10^5	2.8×10^5	1.0×10^5	158.86	156.84	− 2.02

A_1 and E_1 were calculated values; A_2 and E_2 were experimental values; △ was the difference between experimental value and calculated value

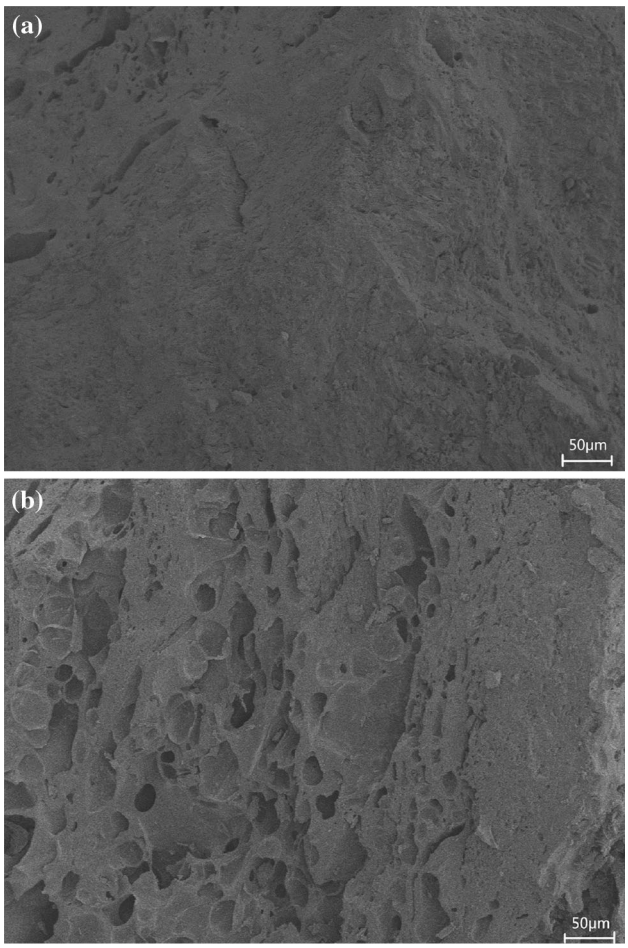

Figure 5 SEM images showing microstructure of fuels. **a** Microstructure of coke; **b** microstructure of charcoal.

gasification of the fuel and therefore accelerated the reactions. This led to the better reactivity of the charcoal compared with the coke, so the higher the content of the charcoal in the mixed fuel, the earlier the reaction start time and the faster the weight loss rate.

By comparing the difference between the experimental and predicted values of the reaction rate of mixed fuel, we could see that the charcoal was not only a simple weighted average of fuel reactivity. The results of previous studies showed that alkali metals can promote the catalytic activity of fuel [15, 16], so we focused on the detection of K and Na in coke, mixed fuel and charcoal by EDS. The detection results are shown in Figs. 6 and 7.

As shown in Figs. 6 and 7, alkali metals, K and Na, were distributed throughout the fuels. The K and Na content in coke was obviously less than that in biomass fuel, which suggested that the reactivity of charcoal was better than that of coke due to catalysis by alkali metals. When alkali atoms are coordinated around a C–C bond, the C atom is attracted which elongates the C–C chemical bond and weakens the binding strength, reducing the activation energy of the reaction (catalytic effect) and making the fuel reaction easier [16, 17]. The alkali metal content in the mixed fuel with charcoal and coke at 50:50 was significantly higher than that of coke alone, which made the reaction rate of mixed fuel higher than the

Table 6 The surface area and pore size distribution of fuels

Samples	Specific surface area (m^2 g^{-1})	Pore volume ($\times 10^2$ cc/g)	Pore diameter (nm)
Charcoal	30.628	538.8	28.9690
Coke	7.191	144.2	40.0948

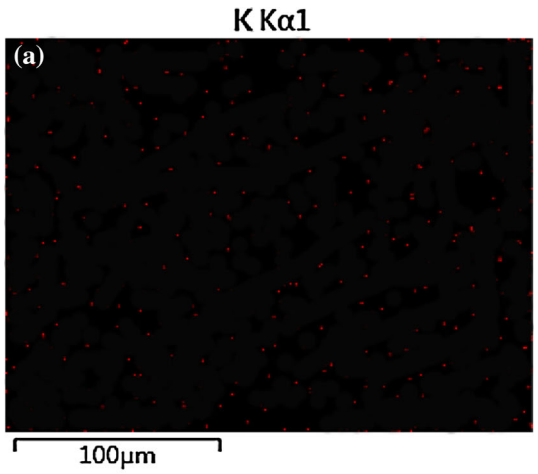

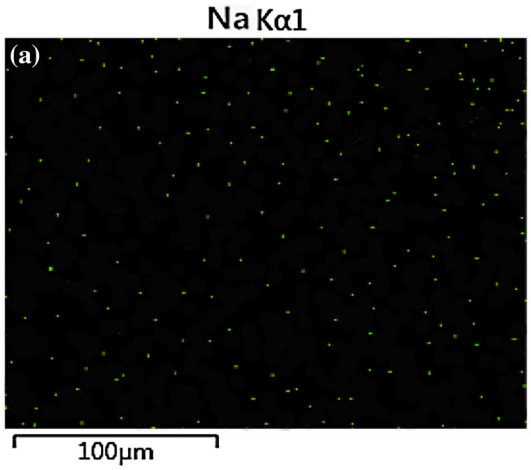

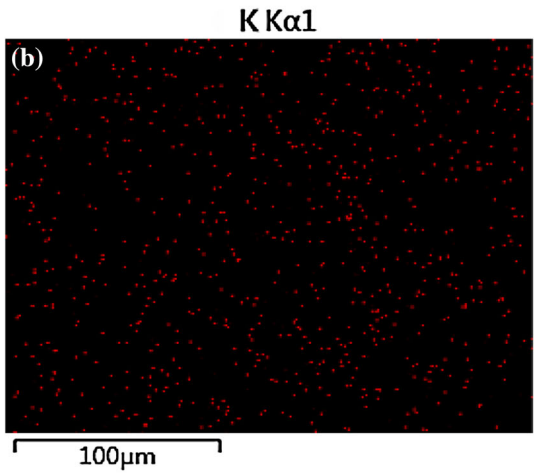

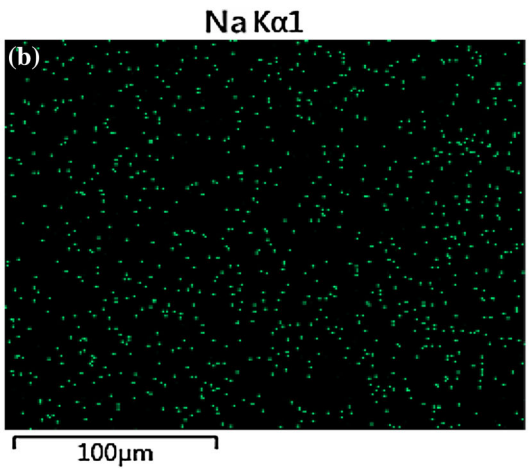

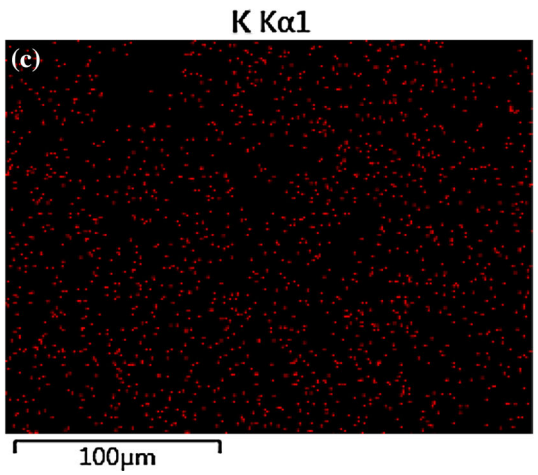

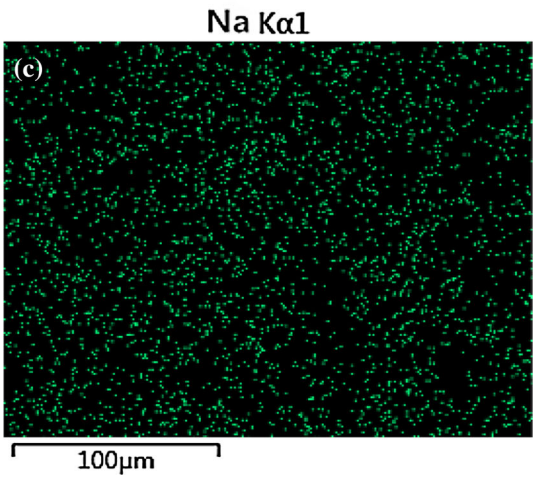

Figure 6 Surface element scanning of K in fuels. **a** K distribution in coke; **b** K distribution in mixed fuel; **c** K distribution in charcoal.

Figure 7 Surface element scanning of Na in fuels. **a** Na distribution in coke; **b** Na distribution in mixed fuel; **c** Na distribution in charcoal.

Table 7 Sintering index and sinter properties

Groups	Vertical sintering rate (mm min^{-1})	Tumbler strength (%)	Yield (%)
1	23.15	65.12	73.16
2	25.82	61.65	72.92
3	29.73	55.39	67.02
4	30.54	50.62	61.88

predicted value, reflecting the catalytic synergism effect of charcoal on mixed fuel reactivity.

Effect of charcoal addition on sinter properties

Sintered cup experiments were carried out according to different schemes in Table 4, and the sintering index and sinter properties were obtained, as shown in Table 7.

The experimental results in Table 7 showed when the content of charcoal substituted coke increased from 0 to 20%, the vertical sintering rate increased from 23.15 to 25.82 mm min^{-1}, the tumbler strength decreased from 65.12 to 61.65%, and the yield changed slightly and kept around 73%. The sinter properties can meet the requirements of iron ore sintering production. However, when the content of charcoal increased from 20% to 60%, the sintering technical indexes began to deteriorate, and the vertical sintering rate increased from 25.82 to 30.54 mm min^{-1}, the tumbler strength and yield decreased from 61.65% and 72.92% to 50.62% and 61.88%, respectively, which were not conducive to the sintering of iron ore powder.

The sinter ore obtained by using different proportion of charcoal instead of coke powder was sliced. The microstructures of sinter ore were examined by Laika phase microscope. Figure 8 shows the results of the microstructures of sinter ore.

Figure 8a is the microstructures of sinter phase obtained by conventional coke sintering. There were a large number of calcium ferrite phase minerals in the figure, and calcium ferrite phase was used as the ideal bonding phase in sinter. The higher the content of calcium ferrite phase was, the better the tumbler strength and reductivity of sinter were. Figure 8b shows the microstructure of sinter phase obtained by 20% charcoal and 80% coke. The content of calcium ferrite decreased and large pores appeared in the

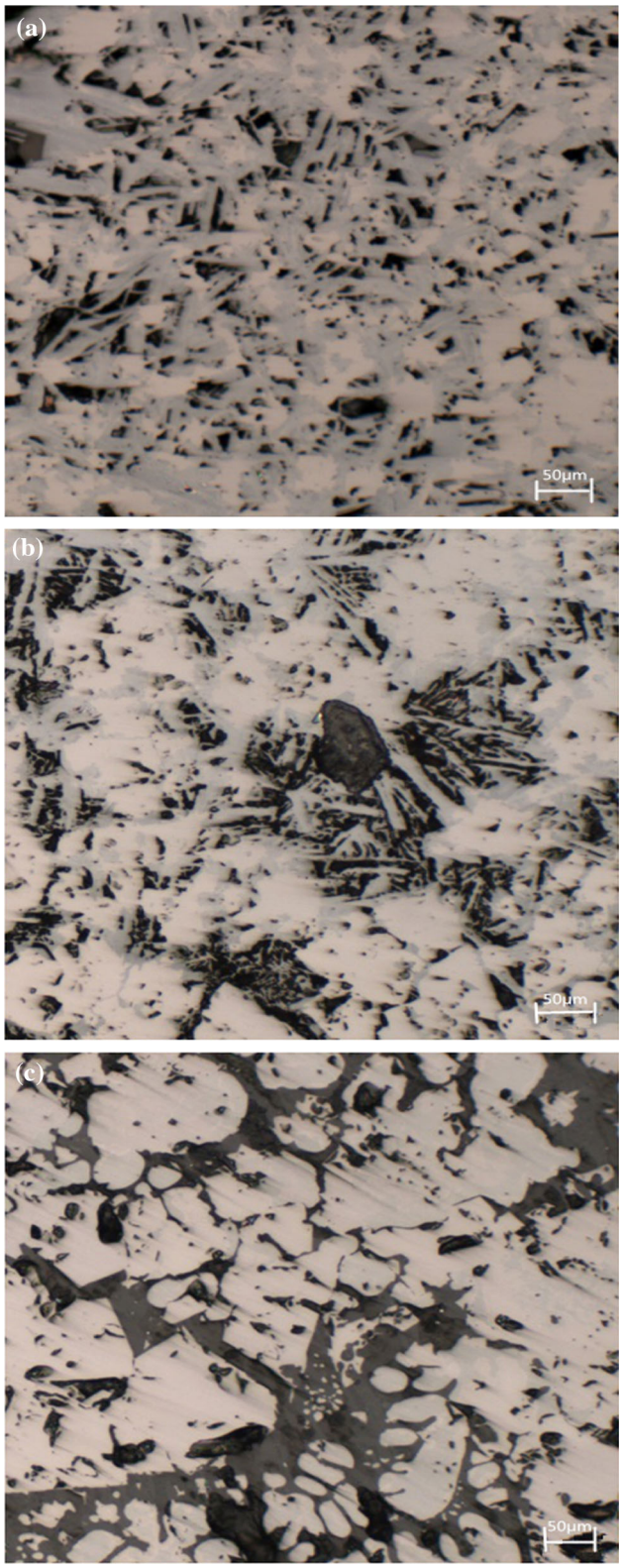

Figure 8 The mineralogical microstructure of sinter ore. **a** 100% Coke; **b** 20% Charcoal + 80% Coke; **c** 40% Charcoal + 60% Coke.

figure, and the distribution was not uniform. In Fig. 8c, the content of bonded phase in sinter decreased, but the calcium ferrite phase was difficult to find. Because the sinter obtained by 60% charcoal and 40% coke had poor strength and was easy to be crushed in the process of sample preparation, no tests had been carried out on the sinter obtained by using 60% charcoal and 40% coke. The results showed that the sinter properties decreased with the increase in charcoal content. Therefore, the reactivity of charcoal should be reduced by reducing the specific surface area and alkali metal content, so as to increase the content of charcoal instead of coke powder to sintering.

Conclusions

1. The combustion and gasification reaction experiments showed that as the biomass fuel content increased, the reaction rate of mixed fuel increased, indicating that biomass fuel can improve the reaction performance of mixed fuel.
2. In the combustion reaction experiment, as the charcoal content increased from 20 to 80%, the reaction time of mixed fuel decreased from 85 to 50 min, and the DTG_{max} increased from 0.58 to 0.72 mg min^{-1}. In the gasification reaction experiment, as the charcoal content increased from 20 to 80%, the pre-exponential factor and activation energy decreased from 4.7×10^6 and 191.08 kJ mol^{-1} to 2.8×10^5 and 156.84 kJ mol^{-1}, respectively.
3. Compared with coke, charcoal has a loose and porous surface structure, which could provide a large specific surface area for the reaction. Biomass fuel also had a higher alkali metal content, which acted as a catalyst and promoted the reactions of mixed fuel. These reasons led to the observed differences between the experimental and the calculated TG and DTG curves, where larger differences are observed with increasing charcoal content.
4. The sintering pot experiment shows that biomass fuel is directly used to replace coke for sintering, the main factor limiting the application of sintering is the reaction performance of biomass fuel, and the sinter properties become worse with the increase in the content of biomass fuel.

Acknowledgements

This research was funded by National Natural Science Foundation of China Grant Number [51874139].

Author contributions

LC participated in experiments and drafted the manuscript. ZYZ conceived and designed the study, performed the statistical analysis, and modified the manuscript. ZK and XHW participated in sintering pot experiments. YAM and KY performed the statistical analysis. All authors read and approved the final manuscript.

Compliance with ethical standards

Conflict of interest The authors declared that they have no conflict of interest.

References

[1] Zhou H, Zhou M, Liu Z, Cheng M, Chen J (2016) Modeling NO_x emission of coke combustion in iron ore sintering process and its experimental validation. Fuel 179:322–331

[2] Adrados A, Marco ID, Solar J, Caballero BM (2015) Biomass pyrolysis solids as reducing agents: comparison with commercial reducing agents. Materials 9(1):3

[3] Liu C, Zhang Y, Shi Y, Xing HW, Kang Y (2017) Numerical simulation of sintering based on biomass fuel. Ironmak Steelmak 5:1–8

[4] Gan M, Fan X, Ji Z, Jinag T, Chen X (2014) Application of biomass fuel in iron ore sintering: influencing mechanism and emission reduction. Ironmak Steelmak 42:27–33

[5] Fan X, Zhiyun JI, Min G, Jiang T, Chen X (2013) Application of biomass fuel in iron ore sintering. J Cent South Univ 44:1747–1753

[6] Kawaguchi T, Hara M (2013) Utilization of biomass for iron ore sintering. ISIJ Int 53:1599–1606

[7] Zandi M, Martinezpacheco M, Fray TAT (2010) Biomass for iron ore sintering. Miner Eng 23:1139–1145

[8] Ooi TC, Thompson D, Anderson DR (2011) The effect of charcoal combustion on iron-ore sintering performance and emission of persistent organic pollutants. Combust Flame 158:979–987

[9] Liu C, Zhang Y, Xing H, Kang Y (2017) Research on performance optimization of biomass fuel for sintering. J Northeast Univ (Nat Sci) 38:1716–1720

[10] He R, Sato J, Chen Q, Chen C (2002) Thermogravimetric analysis of char combustion. Combust Sci Technol 174(4):1–18

[11] Zhang DW, Guo PM, Pei ZHAO (2007) Kinetic study on boudouard reaction of carbon at low temperature. Iron Steel 42:13–16

[12] Hecker WC, Madsen PM, Sherman MR, Allen JW, And RJS, Fletcher TH (2003) High-pressure intrinsic oxidation kinetics of two coal chars. Energy Fuels 17(2):427–432

[13] Liu ZS, Wang Q, Zou ZS, Tan GL (2010) Non-isothermal thermogravimetric investigation on kinetics of coke gasification with CO_2. Res Iron Steel 38:1–3

[14] Sima-Ella E, Yuan G, Mays T (2005) A simple kinetic analysis to determine the intrinsic reactivity of coal chars. Fuel 84:1920–1925

[15] Howaniec N, Smoliński A (2018) Properties of andropogon gerardi derived carbon materials. Materials 11:876

[16] Li X, Hayashi JI, Li CZ (2006) Volatilisation and catalytic effects of alkali and alkaline earth metallic species during the pyrolysis and gasification of Victorian brown coal. Part VII. Raman spectroscopic study on the changes in char structure during the catalytic gasification in air. Fuel 85:1509–1517

[17] He XM, Qin J, Liu RZ, Hu ZJ, Huang CJ (2013) Catalytic combustion of inferior coal in the cement industry by thermogravimetric analysis. Energy Sources 35(13):1233–1240